I&EC research
Industrial & Engineering Chemistry Research

Subscriber access provided by NATIONAL TAIWAN UNIV

Article

Decoupling Multivariable Control with Two Degrees of Freedom

Hsiao-Ping Huang, and Feng-Yi Lin

Ind. Eng. Chem. Res., **2006**, 45 (9), 3161-3173 • DOI: 10.1021/ie051138z

Downloaded from http://pubs.acs.org on November 18, 2008

More About This Article

Additional resources and features associated with this article are available within the HTML version:

- Supporting Information
- Links to the 3 articles that cite this article, as of the time of this article download
- Access to high resolution figures
- Links to articles and content related to this article
- Copyright permission to reproduce figures and/or text from this article

View the Full Text HTML

ACS Publications
High quality. High impact.

Industrial & Engineering Chemistry Research is published by the American Chemical Society. 1155 Sixteenth Street N.W., Washington, DC 20036

Decoupling Multivariable Control with Two Degrees of Freedom

Hsiao-Ping Huang* and Feng-Yi Lin

Department of Chemical Engineering, National Taiwan University, Taipei, Taiwan 10617, Republic of China

A decoupling multivariable control system having two degrees of freedom (2-df) is proposed. The system includes controllers for set-point tracking and for disturbance rejection. Synthesis of an inverse-based multi-input and multioutput (MIMO) decoupler makes use of the zero number deficiency in the adjoint matrix of the process. According to this zero number deficiency, pole(s) and zero(s) are thus introduced to the decoupler to modify the open-loop dynamics and preserve the properness. A new method for synthesizing controllers for disturbance rejection is then presented to design the decoupling controller in the main loop. In addition, model-following and feedforward compensators are incorporated to provide Smith-predictor equivalent capability for set-point tracking. On the basis of the decoupled open-loop process, the controllers for set-point tracking and disturbance are designed independently. Stability robustness of the system can be tuned with two measures for decoupling and model reduction. Robustness of the system to both sensor failure and actuator failure is also included. Simulation examples are used to illustrate the proposed design method. Results from the simulation show that this proposed method is effective for the MIMO control.

1. Introduction

Most chemical processes are mathematically represented by multi-input and multioutput (MIMO) models. To control these MIMO processes, two major approaches have been adopted. One uses multiple single-input single-output (SISO) controllers to constitute a multiloop control system, while the other uses multivariable controllers to become a multivariable control (MVC) system. Because of the fact that multiloop systems are widely used, interactions among loops have been an important issue. Because of the loop interactions, the design of controllers cannot be carried out independently and also the performances of the controllers are confined to some limits. Different methods for designing controllers known as multiloop systems have been proposed (e.g., refs 1−6, etc.). Although these multiloop SISO controllers work well for some cases, the interactions among the loops cannot be eliminated completely. Theoretically, loop interactions can be eliminated by making use of multivariable controllers, that is, the controllers make adjustment to many process inputs simultaneously with access to many feedback variables. For years, MVC has been an important topic for academic research, and extensive papers and books have been published (e.g., refs 7−20, etc.). Lately, design of multivariable variable controllers has been emphasized on obtaining an inverse of the dynamic process model (e.g., refs 21 and 22). In the general controller of Wang et al.,[23] the loop transfer functions are decoupled into several targeting transfer functions, and compensators are designed for step set-point tracking. The resulting system does not perform well in disturbance rejection, which is as important as set-point tracking in process-control applications. Besides, the system designed in that way usually leads to unsatisfactory stability robustness, especially when a Smith predictor is incorporated.[22] The deficiency in disturbance rejection of their controller is due to the fact that their system has only one degree of freedom (df) and, hence, can only be optimally designed for one input (i.e., set point or disturbance) but not for both. This awkwardness can be overcome by a control system that has model following and feedforward from the set point.[24] Nevertheless, the designs of model-following controllers are highly coupled with the controller in the main loop, which may then limit the achievable performance.[20] On the other hand, it is also difficult to tune the feedforward controller as mentioned by Åström and Hägglund.[24] This coupling difficulty in design for SISO systems has been overcome by a double-controller design presented by Tian and Gao,[25,26] as shown in Figure 1. In this system, the two controllers can be designed independently to meet, requiring individual objectives for either set-point tracking or for disturbance rejection. Furthermore, the dead time in the process can also be compensated by incorporating a Smith predictor in their system. Although the configuration works well for SISO systems, it is not trivial to extend it to the control of MIMO systems. The difficulty encountered in the extension is that there needs to be substantial efforts to design two multivariable controllers in two loops, one for set-point tracking and the other for disturbance rejection. Although quite a few methods for MVC design have been reported in the literature with different emphases, it is still not quite mature as far as disturbance rejection is concerned. In this paper, a 2-df multivariable control system is presented. In this 2-df system, incorporated in the main loop is an inverse-based decoupling controller to have good disturbance rejection. In addition, model-following and feed-forward controllers to perform Smith-predictor-type performance for set-point tracking are incorporated. The controllers for two different purposes can be designed independently based on the decoupled open-loop process. Robustness of the system to modeling error as well as integrity is included. Simulation examples are used to illustrate both the design procedures and performances.

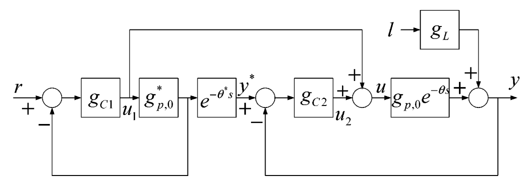

Figure 1. Dual-loop system of Tian and Gao.[25]

2. 2-df Control System for MIMO Processes

The double-controller SISO system of Tian and Gao[25] as shown in Figure 1 can be substantially simplified to a practical configuration, as shown in Figure 2a. It is easy to show that

* To whom correspondence should be addressed. Tel.: 866-2-2363-8999. Fax: 886-2-2362-3935. E-mail: huanghpc@ntu.edu.tw.

10.1021/ie051138z CCC: \$33.50 © 2006 American Chemical Society
Published on Web 03/24/2006

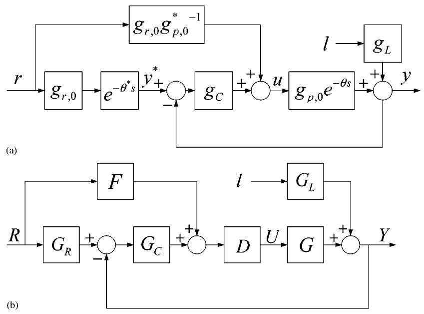

Figure 2. New 2-df control system containing three elements for (a) SISO systems and (b) MIMO systems.

the system in Figure 2a leads to the following equation:

$$y = \frac{g_{\mathrm{r},0}\,\mathrm{e}^{-\theta^* s}\,g_{\mathrm{C}}g_{\mathrm{p},0}\,\mathrm{e}^{-\theta s} + g_{\mathrm{r},0}g_{\mathrm{p},0}^{*\;-1}g_{\mathrm{p},0}\,\mathrm{e}^{-\theta s}}{1 + g_{\mathrm{C}}g_{\mathrm{p},0}\,\mathrm{e}^{-\theta s}}r + \frac{g_{\mathrm{L}}}{1 + g_{\mathrm{C}}g_{\mathrm{p},0}\,\mathrm{e}^{-\theta s}}l \quad (1)$$

Without modeling errors between $g_{\mathrm{p},0}\,\mathrm{e}^{-\theta s}$ and $g_{\mathrm{p},0}^*\,\mathrm{e}^{-\theta^* s}$ (i.e., $g_{\mathrm{p},0}\,\mathrm{e}^{-\theta s} = g_{\mathrm{p},0}^*\,\mathrm{e}^{-\theta^* s}$), the response in eq 1 can be written as follows:

$$y = g_{\mathrm{r},0}\,\mathrm{e}^{-\theta s}\,r + \frac{g_{\mathrm{L}}}{1 + g_{\mathrm{C}}g_{\mathrm{p},0}\,\mathrm{e}^{-\theta s}}l \quad (2)$$

Notice that the system in Figure 2a needs only to specify $g_{\mathrm{r},0}(s)$ for set-point tracking and to design $g_{\mathrm{C}}(s)$ for disturbance rejection. Thus, the design for two controllers in the dual-controller system can be significantly simplified. In the following, the design for the MIMO case will be based on this new control configuration. Consider an $m \times m$ system of the following,

$$Y(s) = G(s)U(s) + G_{\mathrm{L}}(s)l(s) \quad (3)$$

where $Y(s)$ and $U(s)$ designate the output and input vectors and $l(s)$ and $G_{\mathrm{L}}(s)$ represent the load and its transfer function matrix (TFM). Both $G(s)$ and $G_{\mathrm{L}}(s)$ are open-loop stable TFMs as per the following:

$$G(s) = \begin{bmatrix} g_{11}(s) & \cdots & g_{1m}(s) \\ \vdots & \ddots & \vdots \\ g_{m1}(s) & \cdots & g_{mm}(s) \end{bmatrix} \text{ and } G_L(s) = \begin{bmatrix} g_{L1}(s) \\ \vdots \\ g_{Lm}(s) \end{bmatrix} \quad (4)$$

As shown in Figure 2b, the new 2-df control system for the MIMO process consists of a diagonal, $G_{\mathrm{C}}(s)$ (i.e., $g_{\mathrm{C},i}(s)$, $i = 1, 2, ..., m$), and a decoupler, $D(s)$. The $G_{\mathrm{R}}(s)$ represents the targeting TFM for the system to respond to set-point changes, and $F(s)$ is a feedforward compensator. According to the block diagram in Figure 2b, the output of the system can be written as follows:

$$\begin{aligned} Y(s) = \{&(I + G(s)D(s)G_{\mathrm{C}}(s))^{-1}G(s)D(s)G_{\mathrm{C}}(s)G_{\mathrm{R}}(s) + \\ &(I + G(s)D(s)G_{\mathrm{C}}(s))^{-1}G(s)D(s)F(s)\}R(s) + \\ &(I + G(s)D(s)G_{\mathrm{C}}(s))^{-1}G_{\mathrm{L}}(s)l(s) \end{aligned} \quad (5)$$

If $G(s)D(s)F(s)$ is made equal to $G_{\mathrm{R}}(s)$, the above equation for $Y(s)$ becomes

$$Y(s) = G_{\mathrm{R}}(s)R(s) + G_{\mathrm{D}}(s)l(s) \quad (6)$$

where

$$G_{\mathrm{D}}(s) = (I + G(s)D(s)G_{\mathrm{C}}(s))^{-1}G_{\mathrm{L}}(s) \quad (7)$$

It is clear to see from eq 6 that $Y(s)$ depends on $G_{\mathrm{R}}(s)$ and $G_{\mathrm{C}}(s)$ separately. As a result, the design for each part can be conducted independently.

Inversing Decoupler. This decoupler in the main loop is used to decouple the multivariable open-loop process into m individual SISO processes. For this purpose, the process TFM has to be factorized into invertible (i.e., $G_-(s)$) and noninvertible (i.e., $G_+(s)$) parts, that is,

$$G(s) = G_+(s)G_-(s) \quad (8)$$

and the decoupler is formulated as

$$D(s) = G_-^{\;-1}(s)G_{\mathrm{F}}(s) \quad (9)$$

where $G_{\mathrm{F}}(s)$ is a prespecified TFM of filter. But the factorization into the form of eq 8 is not trivial, especially when $G(s)$ has both right-half plane (RHP) zero(s) and different dead times. In general, $G(s)$ is first factorized into two parts:

$$G(s) = \begin{bmatrix} e^{-\theta_1 s} & 0 & 0 \\ 0 & \ddots & 0 \\ 0 & 0 & e^{-\theta_m s} \end{bmatrix} \begin{bmatrix} g_{0,11}(s) & \cdots & g_{0,1m}(s) \\ \vdots & \ddots & \vdots \\ g_{0,m1}(s) & \cdots & g_{0,mm}(s) \end{bmatrix} = \Theta(s)G_0(s) \quad (10)$$

where $\theta_i = \mathrm{Min}\{\theta_{i1}, \theta_{i2}, ..., \theta_{im}\}$.

Provided that $G_0(s)$ is invertible, the decoupler can be designed as

$$D(s) = \{G_0(s)\}^{-1}G_{\mathrm{F}}(s) \quad (11)$$

But the factorization of eq 10 does not guarantee that $G_0(s)$ is invertible, because the determinant of $G_0(s)$, $|G_0(s)|$, may still have dead times and RHP zero(s) as factors. Consequently, identification of the RHP zero(s) of $|G_0(s)|$ is difficult. To circumvent the difficulties encountered in the inversion of $G_0(s)$, the decoupler is given as

$$D(s) = \mathrm{adj}\{G_0(s)\}Z(s) \quad (12)$$

where $Z(s) = \mathrm{diag}\{z_i(s)\}$, $\mathrm{adj}\{G_0(s)\} = [G_0^{ji}(s);\ i, j = 1, 2, ..., m]$, and $G_0^{ij}(s)$ is the cofactor of $g_{0,ij}(s)$. Notice that each diagonal element $z_i(s)$ is given as a simple and stable transfer function. The decoupler in eq 12 is thus open-loop stable, since $G(s)$ is open-loop stable, as has been mentioned. For easy reference, the decoupled process $G(s)D(s)$ is designated as $Q(s)$, that is,

$$Q(s) = G(s)D(s) = \Theta(s)|G_0(s)|Z(s) \quad (13)$$

To implement $D(s)$ of eq 12, each $G_0^{ij}(s)$ is to be replaced by a transfer function in a simpler form, that is,

$$\phi_{ij}(s) = \hat{G}_0^{ji}(s) = \frac{k^{\mathrm{A}}\,\mathrm{e}^{-\delta s}\prod_{i=1}^{n}(\tau_{\mathrm{r},i}^{\mathrm{A}}s + 1)}{(\tau_{\mathrm{p},1}^{\mathrm{A}}s^2 + \tau_{\mathrm{p},2}^{\mathrm{A}}s + 1)\prod_{i=1}^{p}(\tau_{\mathrm{g},i}^{\mathrm{A}}s + 1)} \quad (14)$$

In other words, $\Phi(s)$ is an approximation to $\mathrm{adj}\{G_0(s)\}$. In eq 14, n and p are the number of first-order leads and lags, respectively. In general, $p + 2 - n > 0$. The parameters in the model (i.e., k^{A}, δ, $\tau_{\mathrm{g},i}^{\mathrm{A}}$, $\tau_{\mathrm{r},i}^{\mathrm{A}}$, $\tau_{\mathrm{p},1}^{\mathrm{A}}$, and $\tau_{\mathrm{p},2}^{\mathrm{A}}$) can be obtained by solving the following optimization problem,

$$Arg\{\mathbf{P}\} = \min_{\mathbf{P}} \int_0^{\omega_f} \left\{ \left(\left| \hat{G}_0^{ji}(j\omega) \right| - \left| G_0^{ji}(j\omega) \right| \right)^2 + \left(\measuredangle \hat{G}_0^{ji}(j\omega) - \measuredangle G_0^{ji}(j\omega) \right)^2 \right\} d\omega \quad (15)$$

where $\mathbf{P} = [k^A, \delta, \tau_{g,i}^A, \tau_{r,i}^A, \tau_{p,1}^A$, and $\tau_{p,2}^A]$ and ω_f is a frequency band within which $\hat{G}_0^{ij}(s)$ has a good fit to $G_0^{ij}(s)$. The recommended value of the frequency band is its bandwidth or critical frequency.

To make each element of $D(s)$ realizable, each diagonal element $z_i(s)$ has a number of $N^{ez}[z_i(s)]$ excess zeros. This number is given as the following

$$N^{ez}[z_i(s)] = \min\{N^{ep}[\phi_{ij}(s)], j = 1, 2, ..., m\} \quad (16)$$

where $N^{ep}[\phi_{ij}(s)]$ is the number of excess poles in $\phi_{ij}(s)$ [i.e., $\hat{G}_0^{ji}(s)$].

In eq 13, $|G_0(s)|$ can be implemented by a reduced order form of the following,

$$\varphi(s) = \frac{k^D\, e^{-\theta_{ex}s} \prod_{i=1}^{n} (\tau_{r,i}^D s + 1)}{(\tau_{p,1}^D s^2 + \tau_{p,2}^D s + 1) \prod_{i=1}^{p} (\tau_{g,i}^D s + 1)} = \varphi^0(s)\, e^{-\theta_{ex}s} \quad (17)$$

where $\varphi^0(s)$ is the delay free term of $|G_0(s)|$ and θ_{ex} is the excessive time-delay factorizing from the expansion of $\varphi(s)$. By making use of eq 17, eq 13 can be rewritten into the following,

$$Q(s) \approx \hat{Q}(s) = \varphi^0(s) Z(s) \Theta^*(s) \quad (18)$$

where

$$\Theta^*(s) = \Theta(s) + e^{-\theta_{ex}s} I \quad (19)$$

The diagonal TFM, $\Theta^*(s)$, consists of effective apparent dead times. The same apparent dead times appear also in $G_R(s)$. By reallocating the pole(s) and zero(s) in $\varphi(s)$, $z_i(s)$ provides the availability to modify undesirable dynamic characteristics in $|G_0(s)|$ and, thus, can improve the dynamics resulting from some large time constants or excessive lags.

The decoupler $D(s)$ is thus implemented via the transfer functions of the following:

$$d_{ij}(s) = z_i(s)\phi_{ij}(s) = z_i(s)\hat{G}_0^{ji}(s), \quad \forall i,j \in \{1, 2, ..., m\} \quad (20)$$

From eq 16, $N^{ez}[z_i(s)]$ is computed. Then, the pole(s) and zero(s) polynomials of $z_i(s)$ can be synthesized by simply reallocating the pole(s) and zero(s) of $\varphi^0(s)$. For example, the number $N^{ez}[z_i(s)]$ of the smallest poles in $\varphi^0(s)$ may constitute the zero polynomial of $z_i(s)$.

Disturbance Rejection. With the process TFM given above and from the block diagram in Figure 3, the process output in response to a disturbance $l(s)$ becomes

$$Y(s) = (I + G(s)D(s)G_C(s))^{-1} G_L(s) l(s) \quad (21)$$

Since the main loop has been decoupled, multiple SISO control elements ($g_{C,i}(s)$, $i = 1, ..., m$) can be designed independently.

From eq 18,

and $$q_i(s) = |G_0(s)| z_i(s)\, e^{-\theta_i s} \approx \varphi^0(s) z_i(s)\, e^{-\theta_i^* s} \quad (22)$$

$$y_i(s) = \frac{g_{L,i}(s)}{1 + q_i(s) g_{C,i}(s)} l(s) \approx \frac{g_{L,i}(s)}{1 + \hat{q}_i(s) g_{C,i}(s)} l(s) \quad (23)$$

where

$$\hat{q}_i(s) = \varphi^0(s) z_i(s)\, e^{-\theta_i^* s} = \hat{q}_i^0\, e^{-\theta_i^* s} \quad (24)$$

The controller design for $g_{C,i}(s)$ becomes a SISO control problem. In literature, synthesis of controllers for single-loop systems was usually aimed at set-point tracking, until recently Chen and Seborg[27] provided a design for disturbance rejection. But here, the controller will be synthesized in a more explicit way.

Notice that $\hat{q}_i(s)$ has been factorized into two parts, (i.e., $\hat{q}_i^0(s)$ and $e^{-\theta_i^* s}$). In the same way, so has $g_{L,i}(s)$,

$$g_{L,i}(s) = g_{L,i}^0(s)\, e^{-L_i s} \quad (25)$$

where $g_{L,i}^0(s)$ and $e^{-L_i s}$ are the delay-free parts and the delay parts of $g_{L,i}(s)$, respectively. It is assumed that the open-loop transfer function from the load input to the output is represented by a first-order plus dead time (FOPDT) model of the following:

$$g_{L,i}(s) = \frac{k_{L,i}\, e^{-L_i s}}{\tau_{L,i} s + 1} \quad (26)$$

To synthesize $g_{C,i}(s)$, a targeting response to a step load input can be assigned so that

$$\begin{aligned} y_i(s) &= \{g_{L,i}(s)[1 - g_{d,i}(s)]\} l(s) \\ &= \{g_{L,i}(s)[1 - g_{d,i}^0(s)\, e^{-\theta_i^* s}]\} l(s) \end{aligned} \quad (27)$$

where $g_{d,i}^0(s)$ has two functional forms to define the desired load response for y_i. They are

$$[g_{d,i}^0]_1(s) = \frac{cs + 1}{as^2 + bs + 1} \quad (28)$$

or

$$[g_{d,i}^0(s)]_2 = \frac{1}{bs + 1} \quad (29)$$

Once $g_{d,i}^0(s)$ is specified, $g_{C,i}(s)$ can be synthesized accordingly. That is,

$$g_{C,i}(s) = \frac{1}{\hat{q}_i^0(s)} \frac{g_{d,i}^0(s)}{1 - g_{d,i}^0(s)\, e^{-\theta_i^* s}} \quad (30)$$

By applying the first-order Pade's approximation for $e^{-\theta_i^* s}$ in eq 30, the controller $g_{C,i}(s)$ can be given as

$$g_{C,i}(s) = \frac{g_{f,i}(s)}{\hat{q}_i^0(s)} \frac{g_{d,i}^0(s)(1 + \theta_i^* s/2)}{(1 + \theta_i^* s/2) - g_{d,i}^0(s)(1 - \theta_i^* s/2)} \quad (31)$$

$$g_{f,i}(s) = \frac{1}{(\tau_{f,i} s + 1)^n} \quad (32)$$

where $\tau_{f,i}$ is the filter time constant and has a default value as $0.05\theta_i^*$. In the following, the parameters of $[g_{d,i}^0(s)]_1$ and $[g_{d,i}^0(s)]_2$ regarding different values of $\tau_{L,i}$ in eq 26 will be computed so as to give minimum errors of y_i in terms of an integral of the absolute error (IAE) measure. That is,

$$\begin{Bmatrix} a^* \\ b^* \\ c^* \end{Bmatrix} \text{ or } \{b^*\} = \arg \mathrm{Min}\left\{\int_0^\infty |y_i(\tau)|\, \mathrm{d}\tau \,\middle|\, |h|_i^* = k_i\right\} \tag{33}$$

where $|h|_i^*$ is the peak gain of the ith decoupled single-loop system:

$$|h|_i^* = \max_{\omega} \{|1 - g_{\mathrm{d},i}^0(j\omega)\, \mathrm{e}^{-j\theta_i^*\omega}|\} \tag{34}$$

Typically, the values of these $|h|_i^*$ are assigned in the range of 1.2−2.0 for stability robustness consideration. It is found that $[g_{\mathrm{d},i}^0(s)]_1$ is good for the case where $2 \le \tau_{\mathrm{L},i}/\theta_i^* \le 100$ and $[g_{\mathrm{d},i}^0(s)]_2$ is recommended for the case where $0.1 \le \tau_{\mathrm{L},i}/\theta_i^* < 2$, respectively. The resulting parameters of $[g_{\mathrm{d},i}^0(s)]_1$ in terms of $\tau_{\mathrm{L},i}/\theta_i^*$ as a parameter are shown in Figure 4. These data are correlated into the following functional form,

$$y = p_1x^3 + p_2x^2 + p_3x + p_4 \tag{35}$$

where

$$x = [\ln(\tau_{\mathrm{L},i}/\theta_i^*)]^{\alpha}, \quad \text{and } y = \{a^*, b^*, c^*\} \tag{36}$$

The resulting data are given in Table 1. On the other hand, the parameters of $[g_{\mathrm{d},i}^0(s)]_2$ are given in Table 2. With those data in the tables, the controller can be synthesized accordingly to meet different values of $|h|_i^*$. If $\hat{q}_i^0(s)$ includes RHP zeros, (i.e., $\Pi(1 - \nu_i s)$, $\nu_i > 0$), they will be treated as additional dead times by using the Pade's approximation. So, these RHP zeros become

$$\Pi(1 - \nu_i s) \approx \Pi\{\mathrm{e}^{-2\nu_i s}(1 + \nu_i s)\} = \Pi \mathrm{e}^{-2\nu_i s}\, \Pi(1 + \nu_i s) = \mathrm{e}^{-2\theta_\nu s}\, \Pi(1 + \nu_i s) \tag{37}$$

where

$$\theta_\nu = \sum \nu_i \tag{38}$$

Thus, $\hat{q}_i^0(s)$ containing additional dead time is represented as

$$\hat{q}_i^0(s) = [\hat{q}_i^0]_-(s)\, \Pi(1 - \nu_i s) = [\hat{q}_i^0]_-(s)\, \mathrm{e}^{-2\theta_\nu s}\, \Pi(1 + \nu_i s) \tag{39}$$

Set-point Tracking. As mentioned, the inverse-based controller in the main loop decouples the open-loop process into multiple SISO open-loop processes. As a result, the feedforward compensator $F(s)$ can be synthesized by the following,

$$F(s) = [\hat{Q}^0(s)]^{-1} G_{\mathrm{R}}^{\ 0}(s) \tag{40}$$

where

$$\hat{Q}^0 = \varphi^0(s)Z(s) \tag{41}$$

so that $G(s)D(s)F(s)$ will be made equal to $G_{\mathrm{R}}(s)$ and the output of the system becomes

$$Y(s) = G_{\mathrm{R}}^{\ 0}(s)\Theta^*(s)R(s) \tag{42}$$

where $\Theta^*(s)$ is given by eq 19. Therefore, for set-point tracking, the desired response can be obtained by specifying the elements of $G_{\mathrm{R}}^0(s)$ (i.e., $g_{\mathrm{R},i}^0(s)$) with a transfer function in the form of eq 43:

$$g_{\mathrm{R},i}^0(s) = \frac{[\hat{q}_i^0]_+(s)}{(\tau_{\mathrm{d},1}s + 1)^n(\tau_{\mathrm{d},2}^{\ 2}s^2 + 2\tau_{\mathrm{d},2}\zeta s + 1)} \tag{43}$$

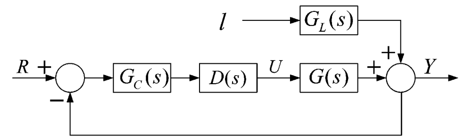

Figure 3. Multivariable decoupling control system.

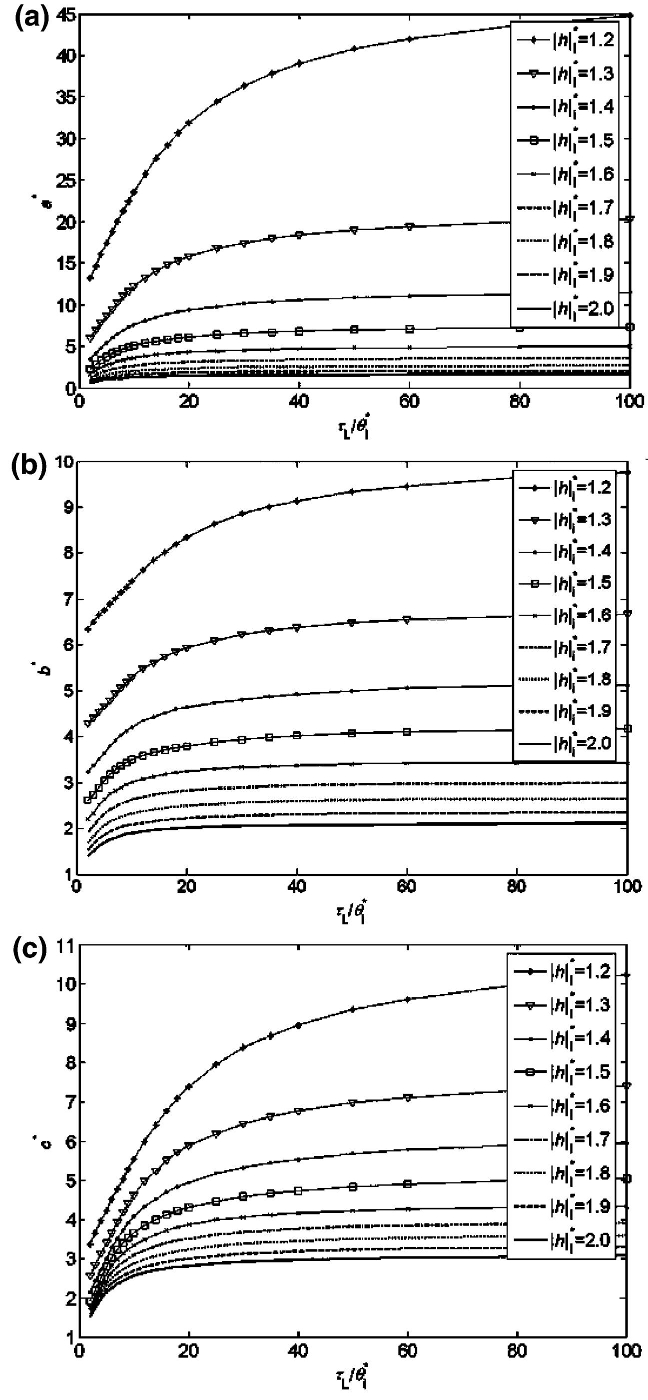

Figure 4. (a), (b), (c) Relations between the parameters of $[g_{\mathrm{d},i}^0(s)]_1$ and $\tau_{\mathrm{L}}/\theta_i^*$ with different values of $|h|_i^*$.

$\tau_{\mathrm{d},i}$ and ζ are the time constant and damping coefficient, respectively, of the second-order model in eq 43. Notice that $[\hat{q}_i^0]_+](s)$ contains all the RHP zeros in $\hat{q}_i^0(s)$. The standard second-order part in eq 43 describes those usual performance requirements, such as overshoot and settling time, etc. The term $(\tau_{\mathrm{d},1}s + 1)^n$ is to provide the necessary high-frequency roll-off rate required. After the desired closed-loop transfer function has

Table 1. Correlation between the Parameters of $[g^0_{d,i}](s)]_1$ and τ_L/θ_i^* for Different $|h|_i^*$ Values

$\lvert h\rvert_i^*$	y	α	p_1	p_2	p_3	p_4
1.2	a^*	3	4.821×10^{-5}	−0.011 12	0.948 2	13.5
	b^*	3	4.504×10^{-6}	−0.001 104	0.1	6.349
	c^*	3	9.575×10^{-6}	−0.002 282	0.201 8	3.397
1.3	a^*	2.3	4.359×10^{-4}	−0.038 43	1.243	5.411
	b^*	2.3	6.103×10^{-5}	−0.005 981	0.207 4	4.14
	c^*	2.3	1.292×10^{-4}	−0.012 16	0.414 2	2.314
1.4	a^*	2	0.001 039	−0.057 53	1.16	2.831
	b^*	2	2.353×10^{-4}	−0.013 52	0.279	3.053
	c^*	2	4.494×10^{-4}	−0.026 01	0.544 9	1.82
1.5	a^*	1.7	0.002 122	−0.082 05	1.142	1.59
	b^*	1.7	7.599×10^{-4}	−0.027 83	0.370 5	2.373
	c^*	1.7	0.001 276	−0.050 09	0.708 8	1.472
1.6	a^*	1.6	0.002 536	−0.081 5	0.943 4	1.055
	b^*	1.6	0.001 034	−0.034 61	0.387 7	1.964
	c^*	1.6	0.001 814	−0.062 43	0.739 4	1.321
1.7	a^*	1.5	0.002 867	−0.079 91	0.799 5	0.727 7
	b^*	1.5	0.001 503	−0.041 7	0.398 2	1.675
	c^*	1.5	0.002 572	−0.075 03	0.763 5	1.215
1.8	a^*	1.4	0.003 261	−0.080 16	0.702 8	0.497 1
	b^*	1.4	0.001 974	−0.047 7	0.403 5	1.455
	c^*	1.4	0.003 384	−0.087 2	0.786 6	1.126
1.9	a^*	1.3	0.003 758	−0.0817 5	0.634 4	0.331 8
	b^*	1.3	0.002 416	−0.054 19	0.413 6	1.271
	c^*	1.3	0.004 192	−0.100 2	0.816 3	1.041
2.0	a^*	1.3	0.002 832	−0.063 59	0.498	0.271 6
	b^*	1.3	0.003 421	−0.062 79	0.411 2	1.138
	c^*	1.3	0.005 213	−0.107 3	0.787 4	1.022

Table 2. Correlation between the Parameters of $[g^0_{d,i}(s)]_2$ and τ_L/θ_i^* for Different $|h|_i^*$ Values

$\lvert h\rvert_i^*$	b^*
1.2	3.499 4
1.3	2.056 4
1.4	1.352 7
1.5	0.937 9
1.6	0.663 7
1.7	0.466 8
1.8	0.314 4
1.9	0.184 1

been specified, the feedforward element $F(s)$ is synthesized as $[\hat{Q}^0(s)]^{-1}G_R{}^0(s)$. The control structure becomes the one as shown in Figure 2b. Notice that $g^0_{R,i}(s)$ must include the RHP zeros of $\hat{q}^0_i$ and $g^0_{R,i}(s)/\hat{q}^0_i(s)$ must be proper.

3. Stability and Robustness

Under the presented 2-df control framework, the stability of the system is determined by the main feedback loop. Because each element of the process $G(s)$ in eq 4 is an open-loop stable function, the decoupler $D(s)$ in eq 12 is designed to be open-loop stable. The nominal stability of the system is guaranteed by the following two conditions:

(1) G_C stabilizes $\hat{Q}(s)$ in a simple closed loop.

$$(2)\ \bar{\sigma}\{-G_C(j\omega)[I + \hat{Q}(j\omega)G_C(j\omega)]^{-1}\} \le \frac{1}{\underset{\omega}{\mathrm{Max}}\{\bar{\sigma}[\Delta Q(j\omega)]\}};\quad \forall\omega \in [0, \infty]$$

where $\bar{\sigma}$ denotes the largest singular value. Because the nominal process (i.e., G) has been decoupled and $G_C(s)$ is also diagonal and is designed by the synthesis method, condition (1) is satisfied as those in dealing with a number of m single-loop systems. Because of the approximation made in eq 14, $\hat{Q}(s)$ may not equal $|G_0(s)|\Theta(s)Z(s)$ exactly. As a result, a model error (i.e., $\Delta Q(s)$) originating from this approximation can be estimated without difficulty. In general, $\Delta Q(j\omega)$ is very small

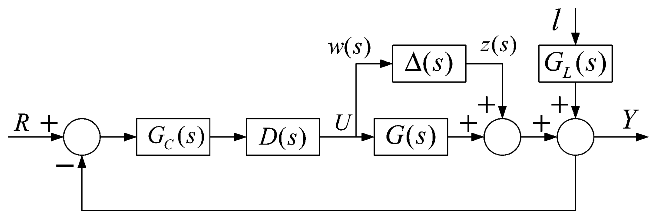

Figure 5. Additive uncertain control system.

in the frequency range concerned for nominal stability, and the second condition can easily be satisfied.

As for stability robustness to modeling error of $G(s)$, consider the control system in Figure 5, where the real process is presented as

$$\tilde{G}(s) = G(s) + \Delta(s) \tag{44}$$

and

$$\bar{\sigma}(\Delta(j\omega)) \le |l(j\omega)| \tag{45}$$

where the perturbation $\Delta(s)$ is bounded on $l(j\omega)$. The system will be robustly stable if

$$\bar{\sigma}[M(j\omega)]|l(j\omega)| < 1, \quad \omega \in [\,0,\infty] \tag{46}$$

where

$$M(s) = -D(s)G_C(s)[I + G(s)D(s)G_C(s)]^{-1} \tag{47}$$

Thus, by selecting an adequate $|h|_i^*$, the controller $G_C(s)$ is synthesized also to satisfy the robust stability in eq 46.

As mentioned, to ensure that eq 46 is met, two types of modeling deficiencies must be taken into consideration. One is due to the approximations for both $\mathrm{adj}\{G_0(s)\}$ and $|G_0(s)|$. The other is due to the modeling error of the process. Because of the aforementioned approximations, a transfer function matrix for the effectiveness of decoupling is considered as the following:

$$\Gamma(s) = G(s)D(s)[\hat{Q}^0(s)]^{-1}G^0_R(s) = \{\gamma_{ij};\ i, j = 1, 2, ..., m\} \tag{48}$$

On the basis of $\Gamma(s)$, an index is defined to indicate the effectiveness of decoupling,

$$D^d_{ji} = \max_{\omega}\left(\frac{|\gamma_{ji}(j\omega)|}{|\gamma_{ii}(j\omega)|}, i \ne j\right), \quad \forall\omega \in [0, \omega_{g,i}\,] \tag{49}$$

where $\omega_{g,i}$ is the frequency where $|\gamma_{ii}(j\omega_{g,i})| = 0.707$.

Notice that D^d_{ji} emphasizes the discrepancy of the off-diagonal elements of $\Gamma(s)$ from zero. This value is mainly determined by the bandwidth of good approximation of $\phi_{ij}(s)$ to the cofactor G_0^{ji}. If the value is too high to be satisfactory, the model order of $\phi(s)$ can be increased. In other words, D^d_{ji} serves as a tuning factor to improve the stability robustness of the system. For good stability robustness, it is recommended that D^d_{ji} is no greater than 0.3.

On the other hand, an index (i.e., $\epsilon_{p,i}$) which measures the discrepancy between the desired and the estimated transfer functions form set point to output is also defined as follows,

$$\epsilon_{p,i} = \max_{\omega}\left\{\frac{|\,|\gamma^d_{ii}(j\omega)| - |\gamma_{ii}(j\omega)|\,|}{|\gamma_{ii}(j\omega)|}, \omega \in [0, \omega_{g,i}]\right\} \tag{50}$$

where

$$\gamma^d_{ii}(s) = g^0_{R,i}(s)\, e^{-\theta_i^* s} \tag{51}$$

The recommended value of the above $\epsilon_{p,i}$ is <0.3. Based on these criteria, the desired decoupling performance, loop performance, and robust stability can be achieved by tuning the parameters of $G_R(s)$ and $G_C(s)$.

Robustness to Sensor Failure. There are two types of sensor failure considered here. One is that some sensor is broken, and the other is that some sensor malfunctions with an additional bias. In the case of a sensor being broken, the characteristic function of the system becomes

$$\det\{I + G(s)D(s)G_C(s)\tilde{I}^i\} = 0 \qquad (52)$$

where $\tilde{I}^i$ denotes an identity matrix with its ith diagonal element being removed. Since $G(s)D(s)G_C(s)$ is a diagonal matrix, the product of $G(s)D(s)G_C(s)\tilde{I}^i$ becomes a diagonal submatrix. As a result, if the nominal case is stable, the system will remain stable, too. Consequently, any sensor broken in this system will not cause stability problem. On the other hand, if some sensor malfunctions with additional biases, it is equivalent to the case where the system has additional but constant unknown inputs as disturbances entering along with the feedback. Since the main loop is designed for dealing with disturbance, these disturbances will not jeopardize the stability in this case.

Robustness to Actuator Failure. In the case of actuator failure, the characteristic equation to be considered becomes

$$\det\{I + G\tilde{I}^i DG_C\} = 0 \qquad (53)$$

where $\tilde{I}^i$ denotes an identity matrix with the ith diagonal element being removed. To retain the system integrity under the conditions of an actuator being broken, G_C in the main loop should be able to stabilize the remaining system. This can be achieved by assigning the proper value to each $|h|_i^*$. With such a G_C, the system still has to be robust to the possible aforementioned modeling errors. For this purpose, eq 46 must also apply to each of the following M^i, that is,

$$M^i(s) = -\tilde{I}^i D(s)G_C(s)[I + G(s)\tilde{I}^i D(s)G_C(s)]^{-1} \qquad (54)$$

4. Illustration with Control of 2 × 2 or 3 × 3 MIMO Processes

In literature, there are quite a few MIMO processes studied for process control. A few of such processes, including those of 2 × 2 and 3 × 3, are used as illustrations of control using the presented design method. The results are compared with those using other methods.

Example 1. Consider the Wood and Berry[28] 2 × 2 process. The transfer function matrices of this process are given as the following:

$$G(s) = \begin{bmatrix} \dfrac{12.8\,e^{-s}}{16.7s+1} & \dfrac{-18.9\,e^{-3s}}{21s+1} \\ \dfrac{6.6\,e^{-7s}}{10.9s+1} & \dfrac{-19.4\,e^{-3s}}{14.4s+1} \end{bmatrix};\quad G_L(s) = \begin{bmatrix} \dfrac{3.8\,e^{-8.1s}}{14.9s+1} \\ \dfrac{4.9\,e^{-3.4s}}{13.2s+1} \end{bmatrix} \qquad (55)$$

First, $G(s)$ is factorized into two parts:

$$G_0(s) = \begin{bmatrix} \dfrac{12.8}{16.7s+1} & \dfrac{-18.9\,e^{-2s}}{21s+1} \\ \dfrac{6.6\,e^{-4s}}{10.9s+1} & \dfrac{-19.4}{14.4s+1} \end{bmatrix}$$
$$\Theta(s) = \begin{bmatrix} e^{-s} & 0 \\ 0 & e^{-3s} \end{bmatrix} \qquad (56)$$

The Bode's diagrams of $|G_0(s)|$ are as shown in Figure 6. A

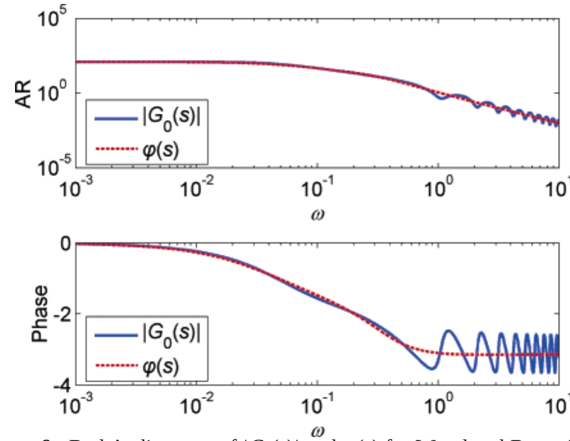

Figure 6. Bode's diagrams of $|G_0(s)|$ and $\varphi(s)$ for Wood and Berry (WB) (2 × 2) process.

rational approximation for $|G_0(s)|$ is found and given in the following:

$$\varphi(s) = \frac{-123.58(1.67s+1)}{(24.75s+1)(8.61s^2+4.52s+1)} \qquad (57)$$

For comparison, the frequency response of this model is also plotted on the same figure.

On the basis of eq 55, the adjoint of $G_0(s)$ is

$$\mathrm{adj}\{G_0(s)\} = \begin{bmatrix} \dfrac{-19.4}{14.4s+1} & \dfrac{18.9\,e^{-2s}}{21s+1} \\ \dfrac{-6.6\,e^{-4s}}{10.9s+1} & \dfrac{12.8}{16.7s+1} \end{bmatrix} \qquad (58)$$

Because each cofactor of $G_0(s)$ has FOPDT dynamics, the number of excess poles for each (i.e., $N^{ep}[G_0^{ji}]$) is one. By eq 16, the number of excess zeros for each element of $Z(s)$, $N^{ez}(z_i)$, is one. Thus, the following simple transfer function is assigned to each of $z_i(s)$ to compensate for undesired poles in the determinant of $G_0(s)$.

$$z_1 = z_2 = (8.61s^2 + 4.52s + 1)/(1.67s + 1) \qquad (59)$$

Thus, the decoupler can be obtained by eq 20. The result is given in Table 3. By the given decoupler, the decoupled open-loop process $\hat{Q}(s)$ is also given in Table 4. Notice that the $\Theta(s) = \Theta^*(s)$ in this case. As required, the desired closed-loop transfer function $G_R^0(s)$ (see Table 4) together with the following are specified:

$$|h|_1^* = 1.3 \quad \text{and } |h|_2^* = 1.8 \qquad (60)$$

Notice that the above values are so chosen that the system can sustain its stability under one broken actuator.

By the resulting values of $\tau_{L,1}/\theta_1^*$ (14.9) and $\tau_{L,2}/\theta_2^*$ (4.4), the following $[g_{d,1}^0(s)]_1$ and $[g_{d,2}^0(s)]_1$ are thus obtained by making use of the data in Table 1:

$$[g_{d,1}^0(s)]_1 = \frac{5.33s+1}{14.33s^2+5.66s+1} \qquad (61)$$

and

$$[g_{d,2}^0(s)]_1 = \frac{6.736s+1}{13.43s^2+6.065s+1} \qquad (62)$$

The results of design are summarized in Tables 4 and 5.

Table 3. Models of Decouplers for 2 × 2 Systems

process	Wood and Berry	Jerome and Ray
$d_{11}(s)$	$\frac{-19.4(8.61s^2+4.52s+1)}{(14.4s+1)(1.67s+1)}$	$\frac{(0.88s+1)(2.9s+1)}{(4s^2+6s+1)}$
$d_{12}(s\}$	$\frac{18.9(8.61s^2+4.52s+1)\,e^{-2s}}{(21s+1)(1.67s+1)}$	$\frac{-0.5(0.88s+1)(2.9s+1)\,e^{-2s}}{(2s+1)(3s+1)}$
$d_{21}(s)$	$\frac{-6.6(8.61s^2+4.52s+1)\,e^{-4s}}{(10.9s+1)(1.67s+1)}$	$\frac{-0.33(0.88s+1)(2.9s+1)\,e^{-3s}}{(4s+1)(5s+1)}$
$d_{22}(s)$	$\frac{12.8(8.61s^2+4.52s+1)}{(16.7s+1)(1.67s+1)}$	$\frac{(0.88s+1)(2.9s+1)}{(s^2+1.5s+1)}$

Table 4. Decoupled Open-Loop Processes, Desired Closed-Loop Transfer Functions, and Feedforward Compensators for 2 × 2 Systems

process	loop 1	loop 2
	Wood and Berry (WB)	
$\hat{q}_i(s)$	$\frac{-123.58\,e^{-s}}{(24.75s+1)}$	$\frac{-123.58\,e^{-3s}}{(24.75s+1)}$
$g^0_{R,i}(s)$	$\frac{1}{4s^2+2.8s+1}$	$\frac{1}{4s^2+2.8s+1}$
$F(s)$	$\frac{-0.008\,091\,9(24.75s+1)}{4s^2+2.8s+1}$	$\frac{-0.008\,091\,9(24.75s+1)}{4s^2+2.8s+1}$
	Jerome and Ray (JR)	
$\hat{q}_i(s)$	$\frac{0.835(-s+1)}{(1.143s^2+2.179s+1)}\,e^{-2s}$	$\frac{0.835(-s+1)}{(1.143s^2+2.179s+1)}\,e^{-3s}$
$g^0_{R,i}(s)$	$\frac{(-s+1)}{(3.24s^2+2.52s+1)}$	$\frac{(-s+1)}{(3.24s^2+2.52s+1)}$
$F(s)$	$\frac{(1.143s^2+2.179s+1)}{0.835(3.24s^2+2.52s+1)}$	$\frac{(1.143s^2+2.179s+1)}{0.835(3.24s^2+2.52s+1)}$

Table 5. Resulting Controllers with Full Forms and Reduced PID Forms for 2 × 2 Systems

process	loop 1	loop 2
	Wood and Berry (WB)	
$g_{c,i}(s)$, Full form	$\frac{-65.96s^3-147s^2-30.58s-1}{886.1s^3+2447s^2+164.4s}$	$\frac{-250.1s^3-214s^2-32.99s-1}{2489s^3+4032s^2+287.7s}$
$g_{c,i}(s)$, Reduced PID form	$-0.0658\left(1+\frac{1}{10.8s}+0.212s\right)\left(\frac{1}{0.185s+1}\right)$	$-0.0556\left(1+\frac{1}{15.96s}+0.963s\right)\left(\frac{1}{0.53s+1}\right)$
	Jerome and Ray (JR)	
$g_{c,i}(s)$, Full form	$\frac{21.91s^4+55s^3+45.55s^2+13.76s+1}{36.64s^4+83.94s^3+49.14s^2+1.832s}$	$\frac{31.98s^4+76.6s^3+58.95s^2+15.87s+1}{65.33s^4+134.3s^3+71.61s^2+2.629s}$
$g_{c,i}(s)$, Reduced PID form	$6.459\left(1+\frac{1}{11.83s}+2.203s\right)\left(\frac{1}{24.77s+1}\right)$	$5.24\left(1+\frac{1}{13.77s}+2.312s\right)\left(\frac{1}{25.1s+1}\right)$

Simulation results for a unit-step set-point change and a unit-step disturbance input are given in Figures 7 and 8, respectively. The results are compared with those from the multivariable Smith predictor of Wang et al.[22] in Figures 7 and 8. The maximum singular values of $M(s)$ in eq 46 of the two systems are compared in Figure 9.

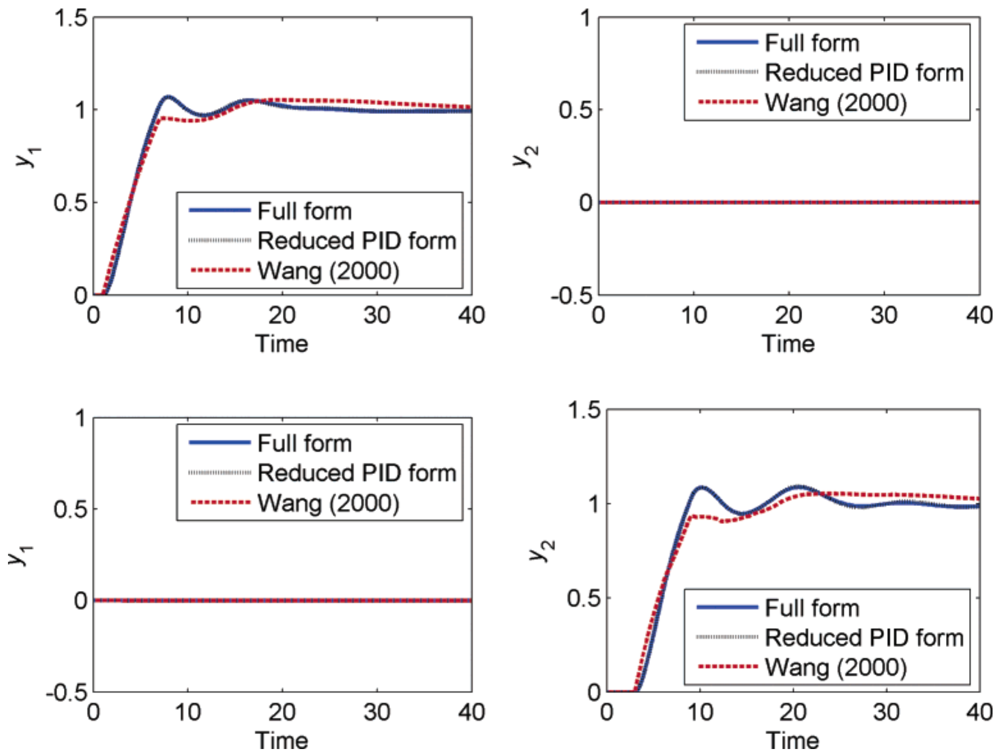

Figure 7. Set-point tracking responses for WB (2 × 2) process.

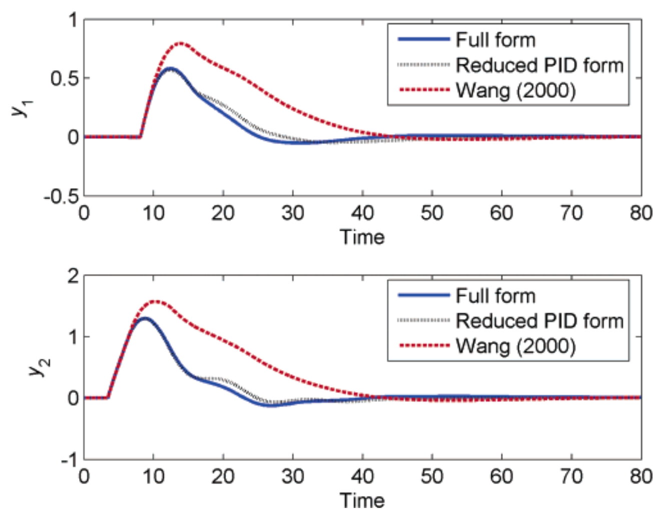

Figure 8. Load rejecting responses for WB (2 × 2) process.

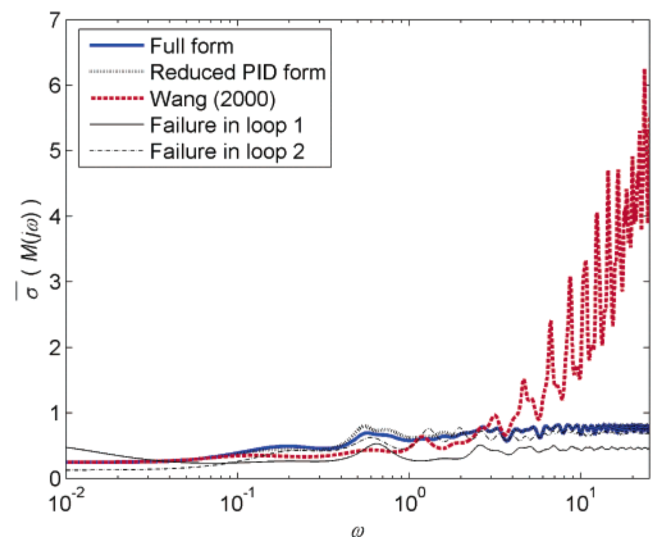

Figure 9. The maximum singular values of $M(s)$ for WB (2 × 2) process.

Example 2. Consider the Jerome and Ray[15] 2 × 2 process. The transfer function matrices of this process are given as the following:

$$G(s) = \begin{bmatrix} \dfrac{(-s+1)\,e^{-2s}}{(s^2+1.5s+1)} & \dfrac{0.5(-s+1)\,e^{-4s}}{(2s+1)(3s+1)} \\ \dfrac{0.33(-s+1)\,e^{-6s}}{(4s+1)(5s+1)} & \dfrac{(-s+1)\,e^{-3s}}{(4s^2+6s+1)} \end{bmatrix} \tag{63}$$

We assume that the disturbance models are

$$G_L(s) = \begin{bmatrix} \dfrac{e^{-s}}{25s+1} \\ \dfrac{e^{-s}}{25s+1} \end{bmatrix} \tag{64}$$

First, $G(s)$ is factorized into two parts:

$$G_0(s) = \begin{bmatrix} \dfrac{1}{(s^2+1.5s+1)} & \dfrac{0.5\,e^{-2s}}{(2s+1)(3s+1)} \\ \dfrac{0.33\,e^{-3s}}{(4s+1)(5s+1)} & \dfrac{1}{(4s^2+6s+1)} \end{bmatrix}$$
$$\Theta(s) = \begin{bmatrix} (-s+1)\,e^{-2s} & 0 \\ 0 & (-s+1)\,e^{-3s} \end{bmatrix} \tag{65}$$

By the proposed design procedure, the inverse-based controllers and the two-element controllers are given in Tables 4 and 5. The simulation results for a unit-step set-point change and a unit-step disturbance input are shown in Figures 10 and 11, respectively. In addition, the maximum singular values of $M(s)$ at different frequencies are given in Figure 12. It can be seen that the 2-df MV control has good performance and robustness.

Example 3. The Tyreus[29] 3 × 3 process as follows is considered.

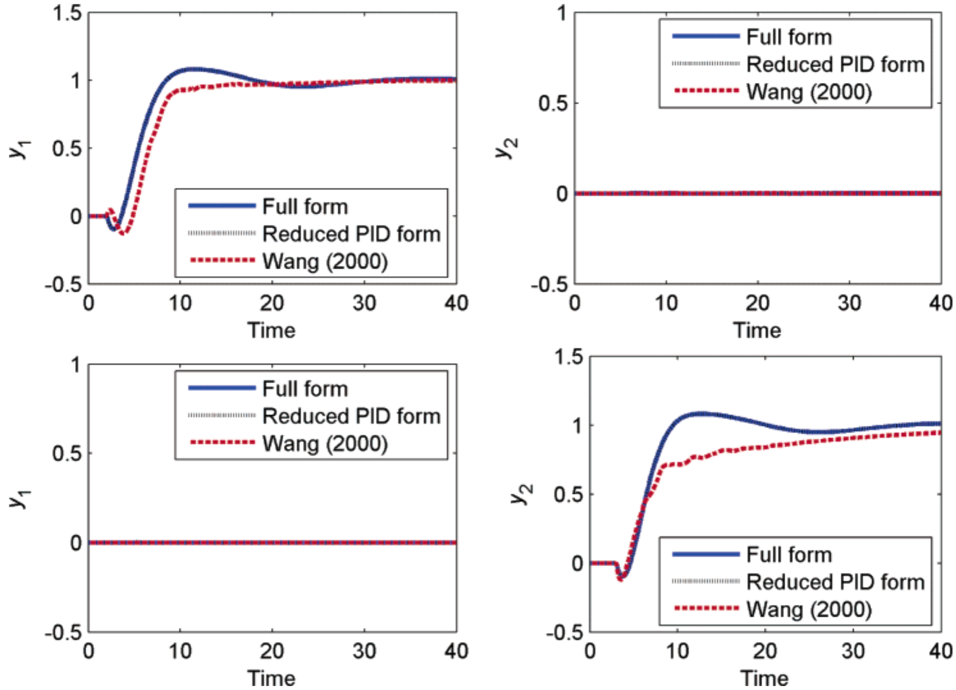

Figure 10. Set-point tracking responses for Jerome and Ray (JR) (2 × 2) process.

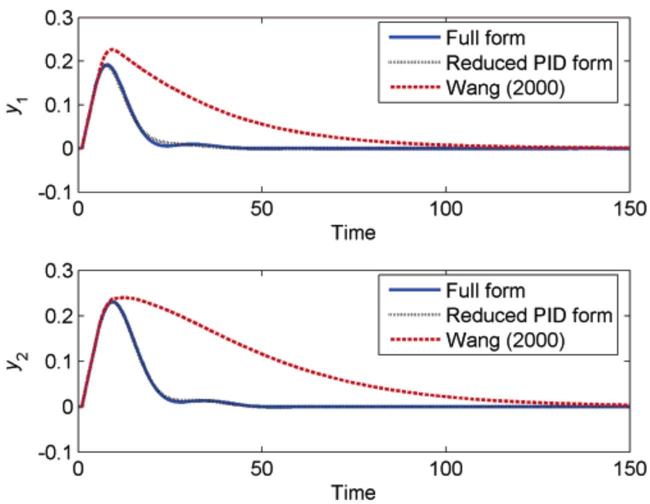

Figure 11. Load rejecting responses for JR (2 × 2) process.

$$G(s)=\begin{bmatrix} \dfrac{1.986\,e^{-0.71s}}{66.7s+1} & \dfrac{-5.24\,e^{-60s}}{400s+1} & \dfrac{-5.984\,e^{-2.24s}}{14.29s+1} \\ \dfrac{-0.0204\,e^{-0.59s}}{(7.14s+1)^2} & \dfrac{0.33\,e^{-0.68s}}{(2.38s+1)^2} & \dfrac{-2.38\,e^{-0.42s}}{(1.43s+1)^2} \\ \dfrac{-0.374\,e^{-7.75s}}{22.22s+1} & \dfrac{11.3\,e^{-3.79s}}{(21.74s+1)^2} & \dfrac{9.811\,e^{-1.59s}}{11.36s+1} \end{bmatrix} \quad (66)$$

Assume the dynamic of disturbance is equal to the first column of $G(s)$, and that is

$$G_L=\begin{bmatrix} \dfrac{1.986\,e^{-0.71s}}{66.7s+1} \\ \dfrac{-0.0204\,e^{-0.59s}}{(7.14s+1)^2} \\ \dfrac{-0.374\,e^{-7.75s}}{22.22s+1} \end{bmatrix} \approx \begin{bmatrix} \dfrac{1.986\,e^{-0.71s}}{66.7s+1} \\ \dfrac{-0.0204\,e^{-3.53s}}{11.49s+1} \\ \dfrac{-0.374\,e^{-7.75s}}{22.22s+1} \end{bmatrix} \quad (67)$$

(i) First, partition $G(s)$ into two parts. They are as follows:

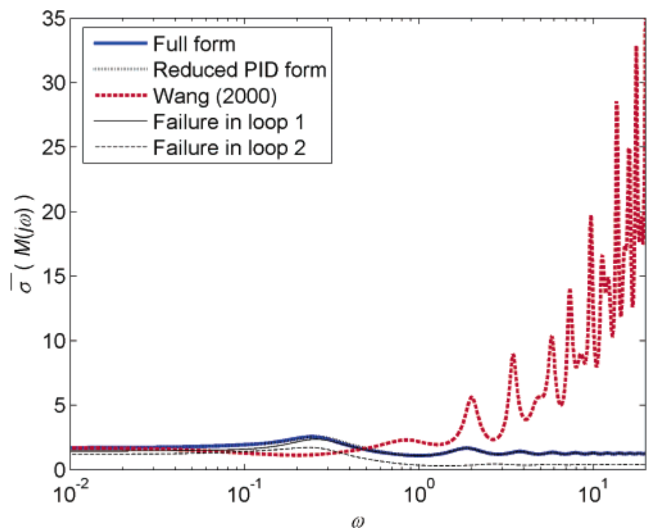

Figure 12. Maximum singular values of $M(s)$ for JR (2 × 2) process.

$$\Theta(s)=\begin{bmatrix} e^{-0.71s} & 0 & 0 \\ 0 & e^{-0.42s} & 0 \\ 0 & 0 & e^{-1.59s} \end{bmatrix}$$

$$G_0(s)=\begin{bmatrix} \dfrac{1.986}{66.7s+1} & \dfrac{-5.24\,e^{-59.29s}}{400s+1} & \dfrac{-5.984e^{-1.53s}}{14.29s+1} \\ \dfrac{-0.0204\,e^{-0.17s}}{(7.14s+1)^2} & \dfrac{0.33\,e^{-0.26s}}{(2.38s+1)^2} & \dfrac{-2.38}{(1.43s+1)^2} \\ \dfrac{-0.374\,e^{-6.16s}}{22.22s+1} & \dfrac{11.3\,e^{-2.2s}}{(21.74s+1)^2} & \dfrac{9.811}{11.36s+1} \end{bmatrix} \quad (68)$$

(ii) Then, approximated models of $|G_0(s)|$ and $G_0^{ij}(s)$ are obtained to give the discrepancy indices at a level of 0.2. The results are as follows:

$$\varphi(s)=\frac{54.77\,e^{-0.26s}}{(1243s^2+75.08s+1)(24.64s+1)(1.171s+1)} \quad (69)$$

Table 6. Desired Closed-Loop Transfer Functions, Resulting Controllers with Full Forms, and Reduced PID Forms for 3 × 3 Systems

process	Tyreus	subsystem of Alatiqi and Luyben
	Loop 1	
$g^0_{\mathrm{R},1}(s)$	$\dfrac{1}{25s^2 + 7s + 1}$	$\dfrac{1}{25s^2 + 7s + 1}$
$g_{c,1}(s)$, Full form	$\dfrac{83.45s^3 + 187.4s^2 + 32.11s + 1}{490s^3 + 1366s^2 + 20.84s}$	$\dfrac{295s^3 + 405.6s^2 + 53.07s + 1}{327.2s^3 + 560s^2 + 26.48s}$
$g_{c,1}(s)$, Reduced PID form	$1.46\left(1 + \dfrac{1}{30.42s} + 6.13s\right)\left(\dfrac{1}{63.69s + 1}\right)$	$2.239\left(1 + \dfrac{1}{59.17s} + 9.762s\right)\left(\dfrac{1}{26.87s + 1}\right)$
	Loop 2	
$g^0_{\mathrm{R},2}(s)$	$\dfrac{1}{64s^2 + 11.2s + 1}$	$\dfrac{1}{25s^2 + 7s + 1}$
$g_{c,2}(s)$, Full form	$\dfrac{37.06s^4 + 151.9s^3 + 136.4s^2 + 29.93s + 1}{4.382s^4 + 146.7s^3 + 524s^2 + 45.29s}$	$\dfrac{589.8s^3 + 551.5s^2 + 56.24s + 1}{688.9s^3 + 863.7s^2 + 24.79s}$
$g_{c,2}(s)$, Reduced PID form	$0.2623\left(1 + \dfrac{1}{11.88s} + 1.05s\right)\left(\dfrac{1}{0.032s + 1}\right)$	$0.6696\left(1 + \dfrac{1}{16.60s} + 0.7650s\right)\left(\dfrac{1}{0.5944s + 1}\right)$
	Loop 3	
$g^0_{\mathrm{R},3}(s)$	$\dfrac{1}{49s^2 + 9.8s + 1}$	$\dfrac{1}{25s^2 + 7s + 1}$
$g_{c,3}(s)$, Full form	$\dfrac{208.5s^3 + 256.7s^2 + 34.71s + 1}{2289s^3 + 3451s^2 + 153.8s}$	$\dfrac{479.4s^3 + 457s^2 + 54.15s + 1}{548.6s^3 + 704.8s^2 + 36.75s}$
$g_{c,3}(s)$, Reduced PID form	$0.0731\left(1 + \dfrac{1}{11.24s} + 0.7137s\right)\left(\dfrac{1}{0.63s + 1}\right)$	$0.7311\left(1 + \dfrac{1}{26.86s} + 0.5167s\right)\left(\dfrac{1}{0.4267s + 1}\right)$

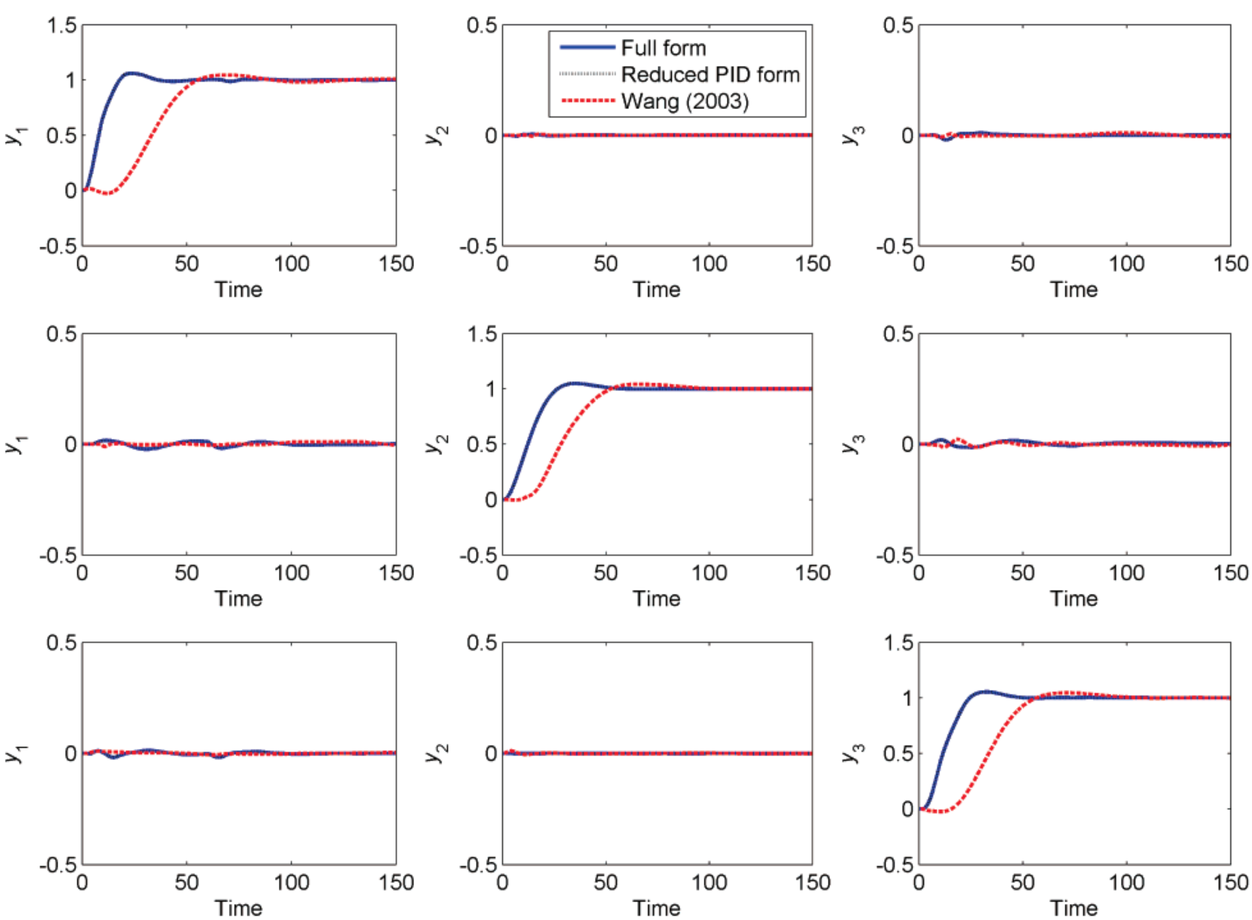

Figure 13. Set-point tracking responses for Tyreus (3 × 3) process.

$$\hat{G}_0^{11}(s) = \frac{30.13\ \mathrm{e}^{-0.2504s}}{(29s+1)(14.97s+1)(1.507s+1)} \tag{70}$$

$$\hat{G}_0^{21}(s) = \frac{-16.21(1645s+1)\ \mathrm{e}^{-4.53s}}{(239.4s^2+24.75s+1)(382.7s+1)(33.80s+1)} \tag{71}$$

$$\hat{G}_0^{31}(s) = \frac{14.45(24.78s+1)\ \mathrm{e}^{-2.232s}}{(415.4s+1)(2.766s+1)^3} \tag{72}$$

$$\hat{G}_0^{12}(s) = \frac{1.09\ \mathrm{e}^{-6.139s}}{(21.06s+1)(0.5274s+1)(3.264s+1)} \tag{73}$$

$$\hat{G}_0^{22}(s) = \frac{17.25(20.31s+1)}{(62.03s+1)(34.80s+1)(5.049s+1)} \tag{74}$$

$$\hat{G}_0^{32}(s) = \frac{4.849}{(64.75s+1)(0.8686s+1)(2.238s+1)} \tag{75}$$

$$\hat{G}_0^{13}(s) = \frac{-0.1071(-33.45s+1)\ \mathrm{e}^{-6.694s}}{(22.65s+1)^2(1.117s+1)(5.277s+1)} \tag{76}$$

$$\hat{G}_0^{23}(s) = \frac{-20.48(7.619s+1)\ \mathrm{e}^{-2.162s}}{(42.78s+1)(42.78s+1)(11.29s+1)(11.27s+1)} \tag{77}$$

$$\hat{G}_0^{33}(s) = \frac{0.5485(418.6s+1)\ \mathrm{e}^{-0.2888s}}{(66.91s+1)(345.4s+1)(2.980s+1)(1.852s+1)} \tag{78}$$

(iii) The compensator $Z(s)$ is used to rearrange the poles-zeros of $|G_0(s)|$, and the resulting $\hat{Q}(s)$ becomes

$$\hat{q}_1 = \frac{54.77\ \mathrm{e}^{-0.97s}}{(24.64s+1)} \tag{79}$$

$$\hat{q}_2 = \frac{54.77\ \mathrm{e}^{-0.68s}}{(24.64s+1)(1.171s+1)} \tag{80}$$

$$\hat{q}_3 = \frac{54.77\ \mathrm{e}^{-1.85s}}{(24.64s+1)} \tag{81}$$

(iv) The desired set-point responses are given in Table 6.

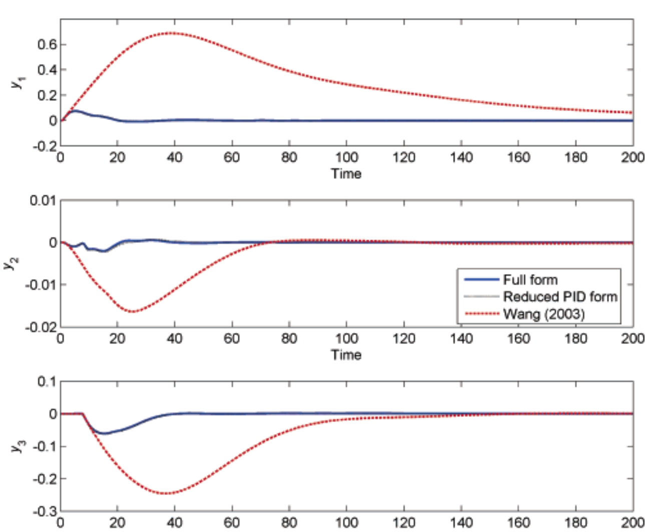

Figure 14. Load rejecting responses for Tyreus (3 × 3) process.

(v) The following indices resulted, $D_{21}^{\mathrm{d}} = 2.71\%$, $D_{31}^{\mathrm{d}} = 4.02\%$, $D_{12}^{\mathrm{d}} = 16.83\%$, $D_{32}^{\mathrm{d}} = 18.29\%$, $D_{13}^{\mathrm{d}} = 16.0\%$, and $D_{23}^{\mathrm{d}} = 0.35\%$; and discrepancy indices, $\epsilon_{\mathrm{p},1} = 10.22\%$, $\epsilon_{\mathrm{p},1} = 7.97\%$, and $\epsilon_{\mathrm{p},1} = 5.78\%$.

(vi) To satisfy robust stability, the value of $|h|_i^*$ for each loop is thus selected as 1.3, and $g_{\mathrm{C},i}$ and reduced proportional−integral−derivative (PID) controllers are obtained as shown in Table 6.

Simulation results for a unit-step change in set point are given in Figure 13. The responses for load rejection are also shown in Figure 14.

Example 4. Consider another subsystem of the 4 × 4 process of Alatiqi and Luyben[30] as the following:

$$G(s) = \begin{bmatrix} \dfrac{4.09\ \mathrm{e}^{-1.3s}}{(33s+1)(8.3s+1)} & \dfrac{-6.36\ \mathrm{e}^{-0.2s}}{(31.6s+1)(20s+1)} & \dfrac{-0.25\ \mathrm{e}^{-0.4s}}{21s+1} \\ \dfrac{-4.17\ \mathrm{e}^{-4s}}{45s+1} & \dfrac{6.93\ \mathrm{e}^{-1.01s}}{44.6s+1} & \dfrac{-0.05\ \mathrm{e}^{-5s}}{34.5s+1} \\ \dfrac{-1.73\ \mathrm{e}^{-17s}}{13s+1} & \dfrac{5.11\ \mathrm{e}^{-11s}}{13.3s+1} & \dfrac{4.61\ \mathrm{e}^{-1.02s}}{18.5s+1} \end{bmatrix} \tag{82}$$

$$G_{\mathrm{L}}(s) = \begin{bmatrix} \dfrac{-0.25\ \mathrm{e}^{-0.4s}}{21s+1} \\ \dfrac{-0.05\ \mathrm{e}^{-5s}}{34.5s+1} \\ \dfrac{4.61\ \mathrm{e}^{-1.02s}}{18.5s+1} \end{bmatrix}$$

Notice that it is assumed that the disturbance enters along with u_3.

In the same way, the 2-df controllers are designed by the proposed design methods for this case. The desired set-point tracking responses are selected so that the decoupling performance indices are 0.2. Then, the inverse-based controllers are synthesized to have $|h|_1^* = 1.3$ and $|h|_2^* = |h|_3^* = 1.4$. The results are summarized in Table 6. Simulation results for a unit-step change in set point and for a unit-step change in load are given in Figures 15 and 16, respectively. The results show that performances of the system are superior to other designs or even better, especially in disturbance rejection.

5. Conclusion

In this paper, a 2-df decoupling multivariable control system and method of design have been proposed. It is capable of dealing with both servo tracking and disturbance rejection. The method to decouple loop interactions is based on fundamental linear algebra without an explicit inverse of the process transfer function. For disturbance rejection, decoupling controllers for a decoupled open-loop process are designed using a proposed new method of synthesis. The achievable set-point tracking response can be easily defined by making use of the resulting loop decoupling. Model-following and feedforward controllers are thus designed based on the decoupled process. The system robust stability can be tuned by selecting $|h|_i^*$ while synthesizing a diagonal element, $G_{\mathrm{C}}(s)$, in the main loop. The selection of $|h|_i^*$ can be made by making use of two proposed measures for decoupling and model reductions. Robustness to the integrity of the system is also included to take account of sensor and actuator failures. Furthermore, the proposed method incorporates dead-time compensation directly in the design. Not only can two objectives be achieved simultaneously while maintaining the minimum loop interactions and desired system robustness, but also their design can be carried out separately. Several

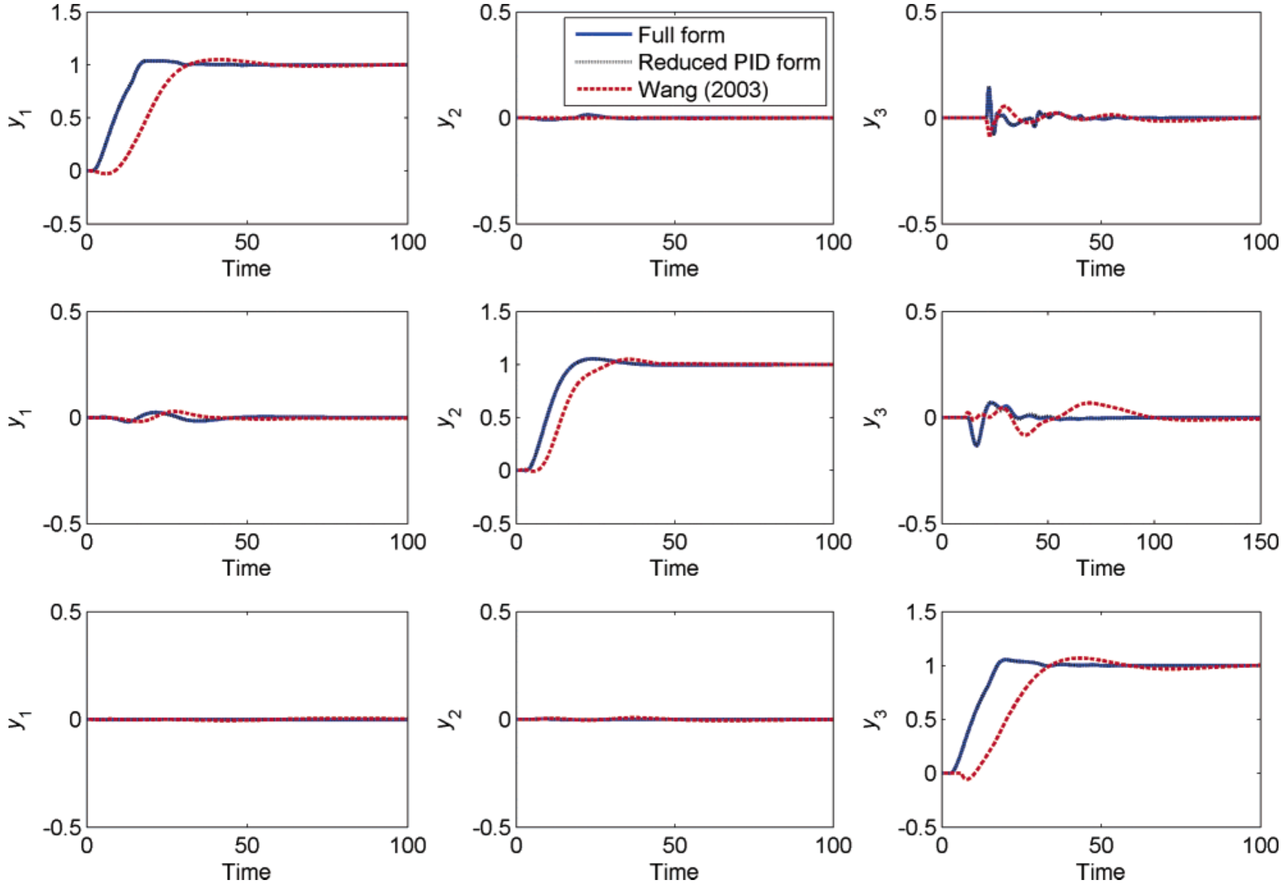

Figure 15. Set-point tracking responses for subsystem of Alatiqi and Luyben (AL) process.

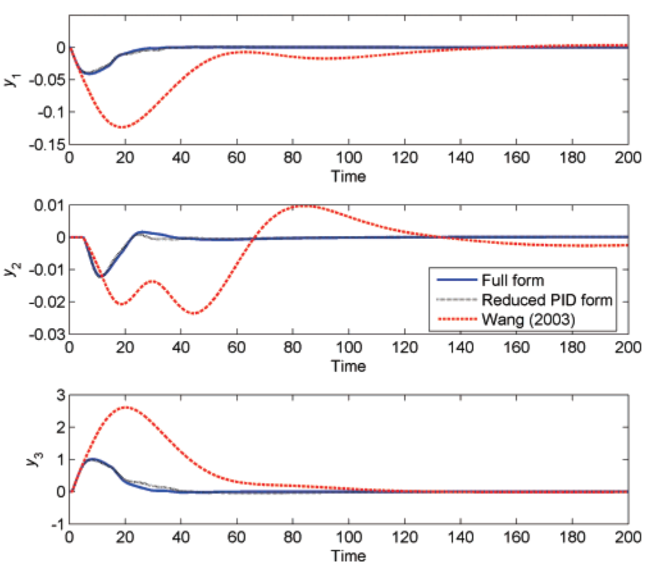

Figure 16. Load rejecting responses for subsystem of AL process.

examples of different dimensions have been used to illustrate the proposed method and its effectiveness in obtaining good performance and robustness.

Acknowledgment

The work is supported by the National Science Council of Taiwan (NSC-93-2214-E−002-008).

Literature Cited

(1) Luyben, W. L. Simple method for tuning SISO controllers in multivariable systems. *Ind. Eng. Chem. Process Des. Dev.* **1986**, *25*, 654.

(2) Yu, C. C.; Luyben, W. L. Design of multiloop SISO controllers in multivariable processes. *Ind. Eng. Chem. Fundam.* **1986**, *25*, 498.

(3) Shen, S. H.; Yu, C. C. Use of relay-feedback test for automatic tuning of multivariable systems. *AIChE J.* **1994**, *40*, 627.

(4) Bao, J.; Lee, P. L.; Wang, F. Y.; Zhou, W. B.; Samyudia, Y. A New Approach to Decentralized Process Control Using Passivity and Sector Stability Conditions. *Chem. Eng. Commun.* **2000**, *182*, 213.

(5) Bao, J.; McLellan, P. J.; Forbes, J. F. A Passivity-Based Analysis for Decentralized Integral Controllability. *Automatica* **2002**, *38*, 243.

(6) Huang, H. P.; Jeng, J. C.; Chiang, C. H.; Pan, W. A direct method for multi-loop PI/PID controller design. *J. Process Control* **2003**, *13*, 769.

(7) Niederlinski, A. A Heuristic Approach to the Design of Linear Multivariable Interacting Control Systems. *Automatica* **1971**, *7*, 691.

(8) Rosenbrock, H. H. *Computer-Aided Control System Design*; Academic Press: New York, 1974.

(9) MacFarlane, A. G. J.; Kouvaritakis, B. A Design Technique for Linear Multivariable Feedback Systems. *Int. J. Control* **1977**, *25*, 837.

(10) Horowitz, I. Quantitative Synthesis of Uncertain Multiple Input-Output Feedback Systems. *Int. J. Control* **1979**, *30*, 81.

(11) Goodwin, G. C.; Ramadge, P. J.; Caines, P. E. Discrete Time Multivariable Adaptive Control. *IEEE Trans. Autom. Control* **1980**, *AC-25*, 449.

(12) Doyle, J. C.; Stein, G. Multivariable Feedback Design: Concepts for a Classical/Modern Synthesis. *IEEE Trans. Autom. Control* **1981**, *AC-26*, 4.

(13) Sinha P. K. *Multivariable control: An introduction*; Marcel Dekker: New York, 1984.

(14) Arulalan, G. R.; Deshpande, P. B. New Algorithm for Multivariable Control. *Hydrocarbon Process.* **1986**, *65*, 51.

(15) Jerome, N. F.; Ray, W. H. High Performance Multivariable Strategies for Systems Having Time Delay. *AIChE J.* **1986**, *32*, 914.

(16) Stein, G.; Athans, M. The LQG/LTR Procedure for Multivariable Feedback Control Design. *IEEE Trans. Autom. control* **1987**, *AC-32*, 105.

(17) Agamennoni, O. E.; Rotstein, H.; Desages, A. C.; Romagnoli, J. A. Robust Controller Design Methodology for Multivariable Chemical Processes: Structured Perturbations. *Chem. Eng. Sci.* **1989**, *44*, 2597.

(18) Maciejowski, J. M. *Multivariable Feedback Design*; Addison-Wesley: New York, 1989.

(19) Figueroa, J. L.; Agamennoni, O. E.; Desages, A. C.; Romagnoli, J. A. Robust Multivariable Controller Design Methodology: Stability and Performance Requirements. *Chem. Eng. Sci.* **1991**, *46*, 1299.

(20) Skogestad, S.; Postlethwaite, I. *Multivariable feedback control*; John Wiley & Sons: New York, 1996.

(21) Wang, Q. G.; Zou, B.; Lee, T. H.; Bi, Q. Auto-tuning of multivariable PID controllers from decentralized relay feedback. *Automatica* **1997**, *33*, 319.

(22) Wang, Q. G.; Zou, B.; Zhang, Y. Decoupling Smith Predictor Design for Multivariable Systems with Multiple Time Delays. *Inst. Chem. Eng.* **2000**, *78*, 565.

(23) Wang, Q. G.; Zhang, Y.; Chiu, M. S. Noninteracting control design for multivariable industrial processes. *J. Process Control* **2003**, *13*, 253.

(24) Åström, K. J.; Hägglund, T. *PID Controllers: Theory, Design, and Tuning*; ISA Press: Research Triangle Park, NC, 1995; p 284.

(25) Tian, Y. C.; Gao, F. Double-controller scheme for separating load rejection from set-point tracking. *Trans. Inst. Chem. Eng.* **1998**, *76*, 445.

(26) Tian, Y. C.; Gao, F. Control of Integrator Processes with Dominant Time Delay. *Ind. Eng. Chem. Res.* **1999**, *38*, 2979.

(27) Chen, D.; Seborg, D. E. PI/PID controller design based on direct synthesis and disturbance rejection. *Ind. Eng. Chem. Res.* **2002**, *41*, 4807.

(28) Wood, R. K.; Berry, M. W. Terminal composition control of a binary distillation column. *Chem. Eng. Sci.* **1973**, *28*, 1707.

(29) Tyreus, B. D. Paper presented at the Lehigh University Distillation Control Short Course, Lehigh University, Bethlehem, PA, 1982.

(30) Alatiqi, I. M.; Luyben, W. L. Control of a complex side stream column/stripper distillation configuration. *Ind. Eng. Chem. Process Des. Dev.* **1986**, *25*, 762.

Received for review October 12, 2005
Revised manuscript received January 13, 2006
Accepted February 6, 2006

IE051138Z